

An update on the Kappa

D.V. Bugg

Queen Mary, University of London, London E1 4NS, UK

Abstract

New FOCUS data on $D^+ \rightarrow K^- \pi^+ \pi^+$ are fitted to the κ , together with earlier data from LASS, E791 and BES 2. There is a clear low mass $K\pi$ peak due to the κ pole. Inclusion of the $I = 3/2$ $K\pi$ amplitude gives only a marginal improvement to the fit and almost no change to the κ peak. An improved formula for the κ gives a better fit than that used earlier. The κ pole moves to $663 \pm 8(stat) \pm 34(syst) - i[329 \pm 5(stat) \pm 22(syst)]$ MeV. The $K_0(1430)$ pole is at $1427 \pm 4(stat) \pm 13(stat) - i[135 \pm 5(stat) \pm 20(syst)]$ MeV.

PACS: 14.40.-n, 13.75.Lb, 11.30.Qc

Keywords: mesons, resonances

1 Introduction

There are two objectives in this paper. The first is to present a fit to new FOCUS data [1] and compare them with earlier E791 data [2]. There are some systematic discrepancies between these two sets of data, although their effects are minor. Like E791, the FOCUS group has determined the $K^- \pi^+$ S-wave amplitude in magnitude and phase in 40 mass bins covering the whole mass range available in $D^+ \rightarrow K^- \pi^+ \pi^+$. These data are fitted here.

The second objective is to introduce a necessary modification to the formula used earlier to fit the κ . Both σ and κ resonances have widths which are strongly s -dependent, giving them unusual features. This s -dependence originates directly from chiral symmetry breaking. Hopefully, the formulae developed here will be useful to experimental groups as direct replacements for the usual Breit-Wigner amplitudes used to fit $J^P = 0^+$ resonances such as κ and $K_0(1430)$ in Dalitz plots. The parametrisation for the $K\pi$ channel is highly convergent and well determined in terms of just three parameters, one of them related closely to f_π^2 . Some allowance is also required for coupling to $K\eta$ and $K\eta'$, but in the absence of direct experimental information on these channels, this requires just one coupling constant for each channel. If data for these channels become available, the present treatment of $K\pi$ could be substituted also for $K\eta$ and $K\eta'$.

2 Formulae

The key point about both σ and κ is the Adler zero in the elastic amplitude at $s \simeq m_K^2 - m_\pi^2/2$ for the κ and at $s \simeq m_\pi^2/2$ for the σ . These zeros are crucial features of chiral symmetry breaking. The mechanism of this symmetry breaking is fully understood [3] [4] [5] and is confirmed in outline by Lattice QCD calculations [6]. References [3-5] give illuminating discussions of the detailed mechanism. Pioneering work on the κ and σ was done by Pelaez, Oset and Oller and collaborators [7] [8] [9] [10].

The consequence of the Adler zero is that the $K\pi$ amplitude rises nearly linearly with s near threshold. In Ref. [11], the κ amplitude was parametrised as a Breit-Wigner amplitude with s -dependent width:

$$f_{el} = \frac{N(s)}{D(s)} = \frac{M\Gamma_{el}}{M^2 - s - iM\Gamma_{total}} \quad (1)$$

$$M\Gamma_{el} = \frac{s - s_A}{M^2 - s_A} \exp(-\alpha k^2) g^2 (K\pi) \rho_{K\pi}(s); \quad (2)$$

here $s_A = 0.2367 \text{ GeV}^2$ is the mean position of the Adler zero for $K^+\pi^-$ and $K^0\pi^0$, and $\rho(s)$ is Lorentz invariant phase space $2k/\sqrt{s}$, where k is centre of mass momentum. Also g are coupling constants and α is a fitted constant. The exponential form factor in (2) accommodates the experimental fact that Γ_{el} gradually flattens off at large s .

There are two weaknesses in these formulae. The important one is that they assume the κ phase shift eventually reaches 90° , although it was found in [11] that this was only at $\sim 3.3 \text{ GeV}$, well above the mass range of available data. The FOCUS data, combined with earlier data, now reveal that the κ phase shift appears to reach only $\sim 55^\circ$ at 1.5 GeV and may never reach 90° . It is straightforward to modify the formulae to cater for this possibility. The second weakness is that the mass and width of the pole itself are far removed from M and Γ_{total} of Eqs. (1) and (2), for reasons described in Section 4. Formulae can be rewritten to be more closely related to the κ pole itself.

A better form of the equations may be obtained by dividing both numerator and denominator of eqn. (1) by M^2 and writing

$$f_{el} = \frac{b_1(s - s_A)F_1(s)\rho_{K\pi}(s)}{1 - s/M^2 - i\sum_j b_j(s - s_{A_j})F_j(s)\rho_j(s)}. \quad (3)$$

For the κ , the term s/M^2 is small; b_j are constants and the summation in the denominator is over $j = 1 - 3$ for $K\pi$, $K\eta$ and $K\eta'$ channels in principle, though the coupling to $K\eta$ turns out to be insignificant. Form factors F_j are discussed in detail below.

Weinberg predicted the scattering lengths of pions from any target [12]; this sets the scale of chiral symmetry breaking, hence b_1 in terms of f_π^2 . Eq. (3) can be recast so as to expose the scattering length explicitly. This requires a transformation in s of the denominator of (3). The algebraic manipulations are to write $1 - s/M^2 = 1 - As \simeq [1 - A(s - s_{thr})]/(1 + As_{thr})$ for small A , next multiply top and bottom of (3) by $(1 + As_{thr})$ then replace all b_j by $B_j = b_j(1 + As_{thr})$; here s_{thr} are evaluated at the threshold of each channel j . The result is

$$f_{el} = \frac{N(s)}{D(s)} = \frac{B_1(s - s_A)F_{el}\rho_{K\pi}(s)}{1 - A(s - s_{thr}) - i\sum_j B_j(s - s_{A_j})F_j(s)\rho_j(s)}. \quad (4)$$

If A is positive, $Re D$ eventually goes to zero and the elastic phase shift reaches 90° . The case where A is negative accommodates the possibility that the phase shift does not reach 90° . The denominator however still allows a κ pole. The scattering length a is

$$a = 2B_1(s_{thr} - s_A)/\sqrt{s_{thr}}. \quad (5)$$

There is an alternative way of viewing this formula. The factor $1 - A(s - s_{thr})$ in the denominator of Eq. (4) may be regarded as an empirical form which exhibits the scattering

length explicitly and parametrises successfully the real part of the amplitude in a region close to threshold and the Adler zero. For elastic scattering, a form factor allowing a controlled departure of the numerator $N(s)$ from linearity is $F_1 = \exp(-\alpha_1 k_1^2)$, where α_1 is a fitted parameter. Note that the exponential dependence of the form factor combines both a conventional form factor for the radius of interaction and an empirical departure of the numerator from linearity; values of α_1 and A are accurately determined by FOCUS and E791 data.

The $K\eta$ channel turns out to be negligible; for $K\eta'$, the Adler zero is at $s = m_{\eta'}^2 - m_K^2/2$. The form factor for $K\eta'$ is not known, because of lack of data for this channel. Above its threshold, the value $\alpha_j = 4.5$ (GeV/c) $^{-2}$ is adopted from a wide range of Crystal Barrel and BES II data; this value corresponds to a reasonable radius of interaction 0.72 fm. Above the $K\eta'$ threshold, small changes in α_j may be taken up by small alterations to parameters fitted to $K_0(1430)$ and $K_0(1950)$ and the fit to data changes by less than the errors.

Below the inelastic threshold, the Flatté prescription is adopted, continuing ρ analytically: $\rho \rightarrow i|\rho|$ [13]. However, $|\rho|$ increases below threshold and requires a cut-off; otherwise, a myriad of open channels at high mass dominate $K\pi$ elastic scattering at low mass. Such a prescription would obviously be unphysical. With the accuracy of present data, any reasonable cut-off will do, and the simple one

$$F_j = \exp[-\alpha_j |k_j^2|] \quad (6)$$

fits data adequately. The best source of information on sub-threshold form factors comes from Kloe data on $\phi \rightarrow \gamma\pi^0\pi^0$, where a similar cut-off is required for the sub-threshold $\sigma \rightarrow KK$ amplitude [14]. Rather a sharp cut-off is required for those data and optimises with $\alpha_j = 8.4$ (GeV/c) $^{-2}$, though a value as low as half this is acceptable. For present data, a similar form factor is definitely required. If a value $\alpha_j < 2$ (GeV/c) $^{-2}$ is used, the $K_0(1430) \rightarrow K\eta'$ amplitude near the $K\pi$ elastic threshold becomes unreasonably large. There is a weak optimum at $\alpha_j = 4.5$ (GeV/c) $^{-2}$. With this value, the sub-threshold contribution rises rapidly from the $K\eta'$ threshold to a $K\pi$ mass of 1400 MeV and thereafter varies slowly and smoothly down to the $K\pi$ threshold. Any alteration to this value of α_j is absorbed by small changes to the fitted parameters of $K_0(1430)$ and small changes to fitted values of α_1 and B_j . The extrapolation of the amplitude to the pole is stable: the real and imaginary parts of the pole position change by 20–30 MeV for variations of α_j in the range 3.5–6.5 (GeV/c) $^{-2}$. This will be taken as a systematic error on the pole position. [If data one day become available on the form factor for $K\eta'$ above threshold, it will be possible to calculate the sub-threshold continuation from a dispersion relation like Eq. (8) discussed below, but presently this is academic.]

For production processes such as $D \rightarrow (K\pi)\pi$, the denominator $D(s)$ of the amplitude must be identical to that of elastic scattering by Watson's theorem [15]. However, the numerator can be (and is) very different. Data on $J/\Psi \rightarrow \omega\pi^+\pi^-$ [16] and $K^+\pi^-K^-\pi^+$ [17] [18] and present data on $D \rightarrow (K\pi)\pi$ may be fitted accurately taking $N(s)$ as a constant. The result is that σ and κ poles appear clearly in production data, but are obscured in elastic scattering by the nearby Adler zero in $N_{el}(s)$. Precise theoretical work on elastic scattering using the Roy equations does however reveal σ and κ poles clearly [19] [20].

The Adler zero is a property of the full $K\pi$ elastic amplitude and therefore needs to be included into the widths of $K_0(1430)$ and $K_0(1950)$. This is done using Eqs. (1) and (2) for each of $K_0(1430)$ and $K_0(1950)$; the exponential form factor is taken to be the same as for the κ . Although $K_0(1430)$ may be fitted with a Breit-Wigner amplitude of constant width, the resulting

contribution to the scattering length is far too large to agree with Weinberg's prediction.

In order to satisfy unitarity for LASS data, the full S-matrices of κ , $K_0(1430)$, $K_0(1950)$ and the $K\pi$ $I = 3/2$ amplitude are multiplied. This prescription is not unique, but gives a good fit to the interference between κ and $K_0(1430)$.

The FOCUS, E791 and BES 2 groups have all determined the magnitude and phase of the $K\pi$ S-wave with respect to other strong components in the data. To fit production data, the isobar model is used, with a complex coupling constant in the numerator of each amplitude instead of $M\Gamma_{el}$, specifically $\Lambda \exp(i\phi)/(M^2 - s - iM\Gamma_{tot})$. The first two sets of data require a phase difference between κ and $K_0(1430) \sim 75^\circ$ different to elastic scattering.

One alternative procedure for fitting the data has been explored, but in practice turns out to give no better result than the Flatté prescription, though it does provide a cross-check. In principle, more complete formulae for a Breit-Wigner resonance are [21]

$$f_{el} = \frac{M\Gamma_{el}}{M^2 - s - m(s) - iM\Gamma_{total}(s)}, \quad (7)$$

$$m(s) = \frac{M^2 - s}{\pi} \int \frac{ds' \Gamma_{total}(s')}{(s' - s)(M^2 - s')}. \quad (8)$$

The scattering amplitude is an analytic function of s . Any s -dependence in $M\Gamma_{total}$ gives rise to a corresponding contribution to the real part of the denominator via $m(s)$. The rapid opening of the $K\eta'$ threshold generates a sharp spike in $m(s)$ precisely at the $K\eta'$ threshold. A subtraction in (8) at mass M improves the convergence of the integral.

The problem which arises is that this spike depends on the mass resolution of the experiments. Without an accurate knowledge of mass resolution and possible variations over the Dalitz plot, inclusion of $m(s)$ is impractical for $K\eta$ and $K\eta'$ channels, though satisfactory for the $K\pi$ channel. The Flatté formula only partially reproduces the effect of $m(s)$. However, in practice, it allows small adjustments of M and $g_{K\eta'}^2/g_{K\pi}^2$ which fudge the effect of $m(s)$ by optimising the fit to data. Readers interested in the effect of $m(s)$ are referred to Ref. [22], where it has been included into fits to $a_0(980)$ in Crystal Barrel data. In that case, the mass resolution is known accurately and included. It smears out the spike at the KK threshold seriously, as shown in Fig. 6(b) of that paper. Even then, the dispersion integral for $m(s)$ is sensitive to the form factor, and the height of the spike needs to be fitted empirically. Here, the dispersive correction will be used for the $K\pi$ channel so as to assess possible systematic errors in parametrising that channel.

3 The fit to data

An important feature of present work is that data from LASS for elastic scattering [23], FOCUS [1] and E791 [2] and BES 2 [18] are fitted simultaneously with consistent parameters. This reveals the strengths and weaknesses of each individual set of data. In BES 2 data, there is a strong $K_0(1430)$ peak, together with a known smaller contribution from the narrower $K_2(1430)$. This peak is included in the present fit since it gives the best determination of parameters for $K_0(1430)$.

The E791 data were published including a form factor in $N(s)$ for production, but it was subsequently shown [24] that the fit optimises with this form factor set to 1. That correction has been applied to data fitted here. FOCUS also take the form factor for production to be

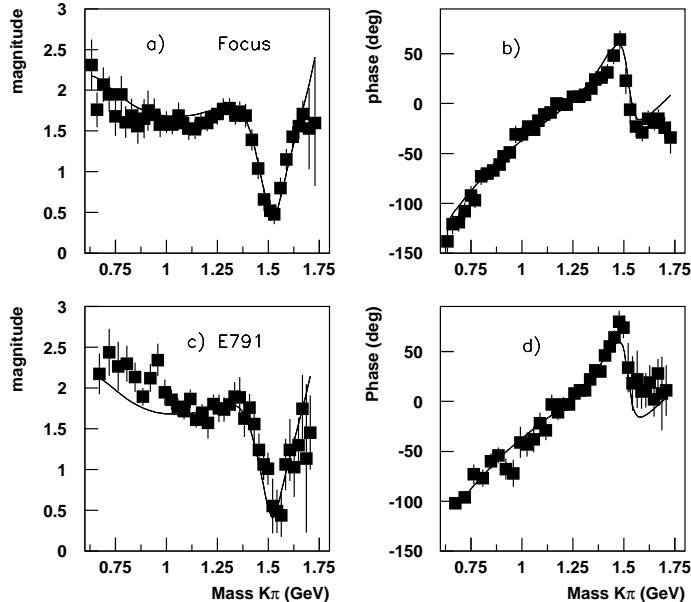


Figure 1: The result of the combined fit for (a) magnitudes and (b) phases of FOCUS amplitudes; (c) and (d) the corresponding fit to E791 data

1. Figs. 1(a)-(d) show the fit to FOCUS and E791 data. One sees some modest systematic discrepancies between them. The fit to either may be improved by omitting the other, but both are included in the final fit. Values of χ^2 will be given for a variety of combinations in Table 2; χ^2 is calculated directly from FOCUS and E791 tabulations, combining their statistical and systematic errors in quadrature.

Figs. 2(a) and (b) show the fit to LASS magnitudes and phases. It is well known that these data stray slightly outside the unitarity circle above 1.5 GeV, so errors in this region have been increased until an average χ^2 of 1 is achieved; this refinement has no significant effect on the fit. Figs. 2(c) and (d) show the fit to BES 2 data. The phases of two high mass points now look high; however, since they are direct measurements of phase in the data, they are retained in the fit. The fit to the 1430 MeV peak in BES 2 data is shown in Fig. 3(a).

The fit to all data requires small contributions from $K_0(1950)$. Its parameters have been allowed to vary by 1σ from averages quoted by the Particle Data Group [25]. They finish at $M = 1967.4$ MeV, $\Gamma_{EL} = 115$ MeV, $\Gamma_{total} = 376$ MeV, but these changes have insignificant effect on parameters fitted to κ and $K_0(1450)$.

There is one quite large change in the fit to $K_0(1430)$ compared to that reported in Ref. [24]. The ratio $g_{K\eta'}^2/g_{K\pi}^2$ reported there was 1.15. This now falls to 0.62 ± 0.06 . This change may be traced directly to the improvement in Eqs. (3-5) over Eqs. (1-2), used earlier. The latter accommodated a $K\pi$ phase of $\sim 72^\circ$ in BES 2 data, but forced a large value of $g_{K\eta'}^2$ for $K_0(1430)$ via the sub-threshold contribution of the $K\eta'$ channel. However, the earlier fit was visibly not perfect from 1.15 to 1.35 GeV because this contribution was too large. That problem

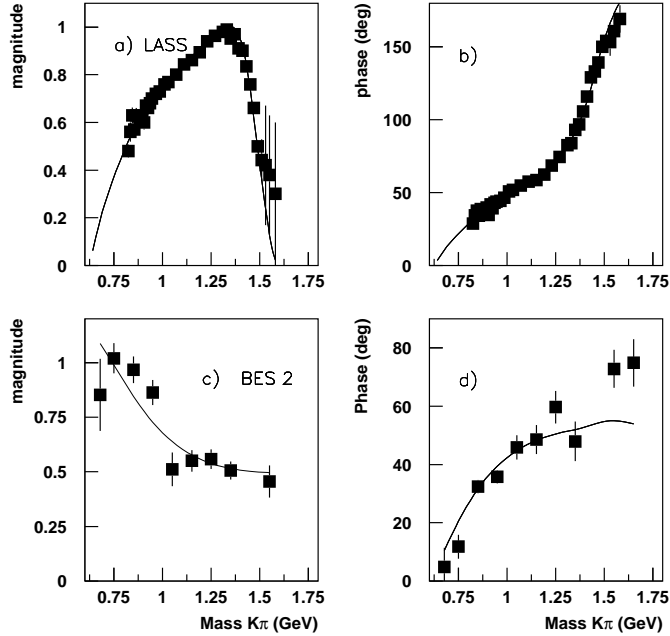


Figure 2: The result of the combined fit for (a) magnitudes and (b) phases of LASS amplitudes; (c) and (d) fits to BES 2 data.

now disappears. With the new formulae, the phase shift of the κ peaks at 55° at 1530 MeV, though any fall between there and the end of the mass range is within statistics. The magnitude and phase of the κ contribution are displayed in Figs. 3(b) and (c). The vertical scale for Fig. 3(b) is arbitrary.

Inclusion of the coupling of κ to $K\eta$ improves χ^2 by only 4.6, i.e. 2σ . It also tends to destabilise the fit because of interferences between the sub-threshold $K\eta$ component and $K\pi$. It is therefore omitted from the final fit. There is now evidence for a component due to $\kappa \rightarrow K\eta'$. It optimises at $g^2(\eta'K)/g^2(K\pi) = 0.085 \pm 0.020$ and improves the fit by 14.6, i.e. 3.8σ . It is not strongly correlated with the contribution from $\kappa \rightarrow K\eta'$. The small structure in the κ phase near 1.5 GeV is due to coupling to $K\eta'$. Direct data on $K\eta'$ would be valuable to improve the determination of the coupling of κ and $K_0(1430)$ to this channel.

3.1 Possible effects of the $K\pi$ $I = 3/2$ amplitude

This amplitude has been parametrised by Pennington. His formula for the K-matrix, quoted in Ref. [26], will be repeated here for completeness:

$$K_{3/2} = \frac{(s - 0.27)}{s_{norm}}(-0.22147 + 0.026637\bar{s} - 0.00092057\bar{s}^2), \quad (9)$$

where $\bar{s} = s/s_{norm} - 1$, $s_{norm} = (m_K^2 + m_\pi^2)$ and s is in GeV^2 . Inclusion of this amplitude improves χ^2 only by 7.7. This is an indication that the data agree well with both the magnitude

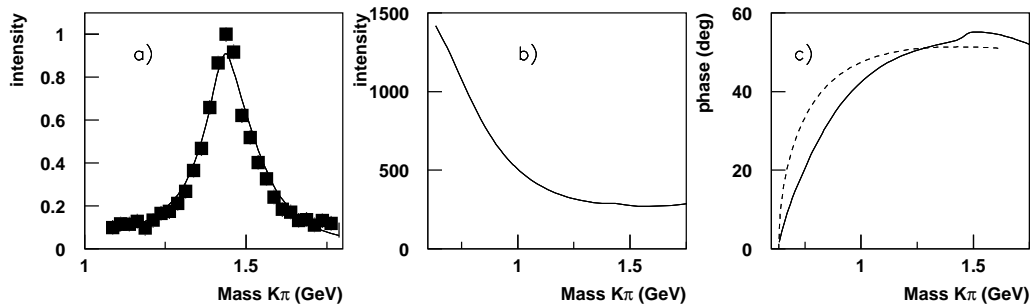


Figure 3: The fit to (a) the intensity of the 1430 MeV peak in BES 2 data; (b) intensity and (c) phase of the fitted κ amplitude. In (c), the dashed curve shows the shape of the LASS effective range formula.

and the phase of the broad κ amplitude. The improvement is not concentrated in any particular mass region or data set, but is fragmented into small improvements distributed almost randomly. What happens in the fit is that destructive interference develops between κ and the $I = 3/2$ amplitude. These are familiar symptoms that two broad amplitudes are combining to fit minor defects in the data.

There is a physics reason why the contribution from repulsive amplitudes should be small. For attractive interactions (particularly resonances), the wave function is sucked into small radii, r ; for repulsive interactions, it is repelled to large r by the potential barrier and therefore reduced in magnitude. There is evidence that J/Ψ and D decays involve short-range interactions. This comes from the absence of form factors in their decay processes. From the earlier analysis of E791 data, the interaction was found to have an RMS radius < 0.38 fm with 95% confidence.

In an earlier FOCUS publication on $D^+ \rightarrow K^- \pi^+ \pi^+$, the repulsive $I = 3/2$ $K\pi$ amplitude was included, but led to massive destructive interference with the κ . In the earlier FOCUS analysis, the Adler zero was not included into the κ amplitude, which was parametrised by a broad Breit-Wigner resonance and a constant interfering background. With three broad amplitudes, destructive interferences are able to patch up minor defects all over the Dalitz plot. Data on other charge combinations could identify production of $I = 3/2$ $K\pi$ and $I = 2$ $\pi\pi$ amplitudes.

The Cleo C collaboration has also presented an analysis of $D^+ \rightarrow K^- \pi^+ \pi^+$ where they include the $I = 2$ $\pi\pi$ amplitude [27]. They present three solutions, all of which contain huge $I = 2$ amplitudes with an intensity a factor ~ 30 larger than $K^*(980)\pi$. This is clearly symptomatic of large destructive interferences with the κ amplitude, since the $K^*(890)$ is clearly visible by eye in the Dalitz plot and $K\pi$ mass projection. Their second solution is made with an amplitude derived directly from a complex pole at $M = 706.0 \pm 1.8(stat) \pm 22.8(syst) - i(319.4 \pm 2.2(stat) \pm 20.2(syst))$ MeV. In view of the huge interference with the $I = 2$ amplitude, it is difficult to know how reliable this result is.

	Parameter	Value
κ	A	-0.080 ± 0.062
	B_1	2.528 ± 0.089
	α_1	0.566 ± 0.056
	$g_{K\eta'}^2/g_{K\pi}^2$	0.085 ± 0.020
$K_0(1430)$	M	1.479 ± 0.004
	$g_{K\pi}^2$	0.284 ± 0.012
	$g_{K\eta'}^2/g_{K\pi}^2$	0.62 ± 0.06

Table 1: Parameters fitted to κ and $K_0(1430)$ in units of GeV

3.2 Pole positions

Table 1 gives fitted parameters for κ and $K_0(1430)$ in units of GeV. Pole positions are remarkably stable if individual sets of data are dropped from the fit, or even pairs of sets. As an illustration, Table 2 shows values when each of the sets of data listed in column 1 are dropped. There are 14 fitted parameters: the 7 listed in Table 1, 6 for three complex coupling constants fitted to κ , $K_0(1430)$ and $K_0(1950)$ in $D \rightarrow K\pi\pi$, and one scale factor for the magnitude fitted to $K_0(1430)$ in BES 2 data. The total χ^2 is 349.4 for 272 degrees of freedom. Errors quoted in Table 1 for each parameter correspond to changes in χ^2 of 1.28, the mean value per degree of freedom. However, there are some correlations between parameters, with the result that the quoted errors overestimate somewhat the changes expected in Table 2. The final two columns in Table 2 show changes in χ^2 when each set of data is dropped and also the number of points dropped.

Dropped	κ	$K_0(1430)$	$\Delta\chi^2$	points
LASS phases	661 -i325	1432-i127	34.9	41
LASS magnitudes	663 -i334	1435-i140	44.9	41
FOCUS magnitudes	663 -i329	1427-i137	41.7	40
FOCUS phases	660 -i327	1427-i129	98.2	40
E791 magnitudes	661 -i328	1426-i135	73.2	38
E791 phases	663 -i329	1424-i139	48.2	38
BES $K_0(1430)$	675 -i341	1431-i144	54.0	29
BES magnitudes	640 -i321	1425-i132	21.3	9
BES phases	657 -i323	1426-i133	27.4	10
FOCUS all	660 -i328	1425-i132	158.4	80
E791 all	662 -i327	1424-i140	126.4	76

Table 2: Pole positions in MeV when individual sets of data are dropped; the last two columns show the change in χ^2 of the fit and the number of points dropped.

Using all sets of data, the $K_0(1430)$ pole position is

$$M = 1427 \pm 4(stat) \pm 13(syst) - i[135 \pm 5(stat) \pm 20(syst)] \text{ MeV}. \quad (10)$$

The systematic error is compounded from the worst case and from uncertainties in relative

contributions of $K_2(1430)$ and $K_0(1430)$ (and their relative phase) to BES 2 data on the 1430 MeV peak. For the κ , the pole position is

$$M = 663 \pm 8(stat) \pm 34(syst) - i[329 \pm 5(stat) \pm 22(syst)] \text{ MeV}. \quad (11)$$

Values for both κ and $K_0(1430)$ supersede earlier determinations in Ref. [24] because of the improvement in the formulae for the κ . For the latter, further systematic errors are included to cover uncertainties in the extrapolation to the pole, estimated by changing form factors and a possible small contribution from the $K\eta$ channel. The κ pole has moved from $750_{-55}^{+30} - i342 \pm 60$ MeV [24] by more than the quoted systematic error on mass because of the improvement in the fitting formulae. A systematic discrepancy with LASS data has been cured. There is no apparent need to increase the flexibility in the fitting formulae, but it is difficult to estimate systematic effects this might have on the κ pole.

The scattering length a for the κ component is given by Eq. (5) except for a small correction from the sub-threshold contribution of $K\eta'$ via the denominator of Eq. (4). For the optimum fit, the κ contributes $0.1860/m_\pi$ to the scattering length, $K_0(1430)$ contributes $0.0086/m_\pi$ and $K_0(1950)$ contributes $0.0002/m_\pi$, i.e. a total of $(0.1950 \pm 0.0060)/m_\pi$. Weinberg [12] predicts $0.172/m_\pi$ and corrections from Chiral Perturbation Theory to order p^4 increase this to $(0.19 \pm 0.02)/m_\pi$ [28]. Experiment and prediction are now in good agreement and experiment is now better than theory.

The κ pole position also now agrees well with the prediction of Descotes-Genon and Mousallam [20] from the Roy equations, $658 \pm 13 - i(278 \pm 12)$ MeV. They considered only the mass range up to 1 GeV and omitted the $K\eta'$ amplitude and its sub-threshold contribution.

For completeness, Table 3 shows additional parameters used in fitting the production data of FOCUS and E791. The experimental groups use $K^*(980)$ as a reference amplitude. Table 3 therefore refers to parameters fitting their tabulated amplitudes for the $K\pi$ S-wave. Table 3 also includes the normalisation factor Λ_{norm} which scales the BES 2 data for $K_0(1430)$.

Parameter	Value
Λ_κ	2.98 ± 0.09
Λ_{1430}	-0.72 ± 0.04
Λ_{1950}	-3.16 ± 0.07
ϕ_κ	130.9 ± 2.3
ϕ_{1430}	53.9 ± 2.6
ϕ_{1950}	26.6 ± 4.1
Λ_{norm}	0.925 ± 0.028

Table 3: Additional parameters fitted to production data.

3.3 A check using the dispersive correction $m(s)$

The s -dependence of $m(s)$ derived purely from the $K\pi$ component of Γ_{total} is shown in Fig. 4, after a subtraction at the $K\pi$ threshold. The fit to data including $m(s)$ is almost indistinguishable from that of Figs 1 and 2. To check the scattering length, it is necessary to fit $m(s)$ to

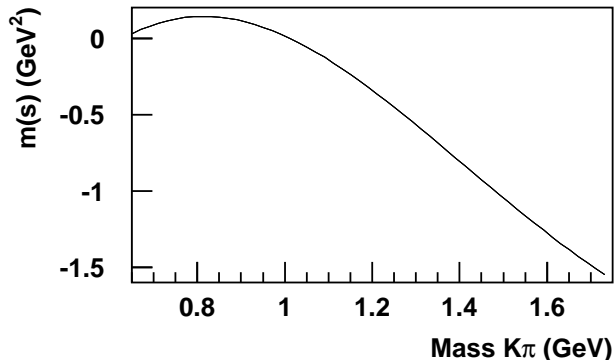


Figure 4: $m(s)$ evaluated from Eq. (8) with a subtraction at the $K\pi$ threshold

terms in k and k^3 . The derived scattering length is $(0.201 \pm 0.007)/m_\pi$, agreeing with the result quoted above within the error. One should note that the dispersion integral for $m(s)$ involves an integral from threshold to infinity and is therefore sensitive to assumptions about the behaviour of the κ amplitude above the available mass range. There could be contributions from further inelastic channels such as $\kappa\sigma$. The $K\pi$ amplitude itself ‘knows’ about such contributions, so the determination of the scattering length direct from fitted amplitudes at low mass is likely to be the more reliable.

3.4 How the κ amplitude varies off the real s -axis

The $K\pi$ and $\pi\pi$ amplitudes are analytic functions of s . From the Cauchy-Riemann relations,

$$\partial(\text{Re } f)/\partial(\text{Re } s) = \partial(\text{Im } f)/\partial(\text{Im } s) \quad (12)$$

$$\partial(\text{Im } f)/\partial(\text{Re } s) = -\partial(\text{Re } f)/\partial(\text{Im } s), \quad (13)$$

there is a rapid variation of both real and imaginary parts of f with $\text{Im } s$. This leads to a rotation of the phase of the amplitude with $\text{Im } s$. On the real s -axis, unitarity requires that the phase is zero at threshold, but it moves negative with increasing negative values of $\text{Im } s$.

This is illustrated in Fig. 5 for four values of $\text{Im } s$. Note the the phase below the pole moves from a small value for the full curve at $\text{Im } m = -0.2$ GeV to a large negative value for $\text{Im } m = -0.32$ GeV, very close to the pole. This explains the curious result that there can be a pole with a real part close to zero at threshold. Oller [29] has drawn attention to this point in a somewhat different way. On the real s -axis, what one sees is similar to the upper part of the pole, but rotated in phase. This explains why the phase for real s does not reach 90° . It reinforces the fact that M and Γ of Eqs. (1) and (2) are remote from those of the pole.

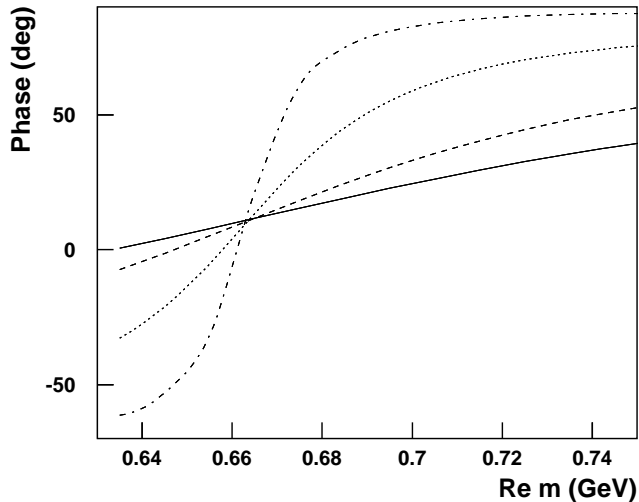


Figure 5: The phase variation near the pole v . mass, for $\text{Im } m = -0.2$ GeV (full curve), -0.25 GeV (dashed), -0.30 GeV (dotted) and -0.32 (chain curve).

4 Discussion of results

The key features emerging from current data are (i) the κ peak near threshold, Fig. 3(b), and (ii) the precise form of the phase shift near threshold, Fig. 3(c). The FOCUS collaboration [1] illustrate in their Fig. 8 the fact that their measured phases near threshold lie distinctly below those obtained from a conventional effective range form. This is of course due to the nearby Adler zero, which is absent from the usual effective range form. The dashed curve in Fig. 3(c) illustrates the LASS effective range formula, which is more curved near threshold.

Insight into the nature of σ and κ is provided by the model of confinement constructed by van Beveren and Rupp [30]. In this simple model, confinement is approximated by a harmonic oscillator potential (which can be solved algebraically), matched to plane wave states at a boundary. The way the model is constructed, it approximately reproduces the effect of the Adler zero. With the boundary at 0.7 fm, the model reproduces quite well the parameters of all of σ , κ , $a_0(980)$ and $f_0(980)$ with a single universal coupling constant. A reasonable phase angle is needed between $u\bar{u}$ and $s\bar{s}$ to reproduce $f_0(980)$ and σ amplitudes near 1 GeV. The $f_0(980)$ and $a_0(980)$ are locked to the KK threshold by the sharp cusp in $m(s)$ due to the opening of this threshold. The $a_0(980)$ does not appear at the $\eta\pi$ threshold because of the Adler zero close to this threshold. It is noteworthy that this model was the first (in 1986) to reproduce the lowest scalar nonet [31], with the title: ‘A low-lying scalar meson nonet in a unitarised meson model’.

In this model, σ , κ , $a_0(980)$ and $f_0(980)$ are a nonet of continuum states coupled to the confining potential at its boundary. They are meson-meson states at large r , coupled to $q\bar{q}$ components within the confining potential. Doubtless the model could be improved by adding meson exchanges at large r . In more detail, it is also possible that diquark interactions play a role via coloured configurations, as proposed by Jaffe [32].

There is a clear analogy between σ and κ and the weak interaction because the amplitude rises linearly with s near threshold. The scale of the electroweak interaction is set by the masses of W and Z . If the Higgs boson appears as a broad pole like σ and κ , dispersive effects due to opening of WW , WZ , ZZ and $t\bar{b}$ thresholds will play an important role [33].

I am grateful for discussions with Profs. G. Rupp, E. van Beveren, P. Bicudo and J. Ribiero over a period of many years.

References

- [1] J.M. Link *et al.*, FOCUS Collaboration, arXiv: 0905.4846, submitted to Phys. Lett. B.
- [2] E.M. Aitala *et al.*, E791 Collaboration, Phys. Rev. D **73** 032004 (2006).
- [3] P. Bicudo and J. Ribiero, Phys. Rev. D **42** 1611 (1990).
- [4] P. Bicudo *et al.*, Phys. Rev. D **65** 076008 (2002).
- [5] A. Höll, A. Krassnigg, C.D. Roberts and S.V. Wright, Int. J. Mod. Phys. A **20** 1778 (2005).
- [6] S. Prelovsek, arXiv:0809.5134.
- [7] A. Dobardo and J.R. Pelaez, Phys. Rev. D **47** 4883 (1993).
- [8] J.A. Oller, E. Oset and J.R. Pelaez, Phys. Rev. D **59** 074001 (1999).
- [9] J.A. Oller and E. Oset, Phys. Rev. D **60** 074023 (1999).
- [10] M. Jamin, J.A. Oller and A. Pich, Nucl. B **587** 331 (2000).
- [11] D.V. Bugg, Phys. Lett. B **572** 1 (2003); erratum Phys. Lett. B **595** 556 (2004).
- [12] S. Weinberg, Phys. Rev. Lett. **17** 616 (1966).
- [13] S. Flatté, Phys. Lett. B **63** 224 (1976).
- [14] D.V. Bugg, Eur. Phys. J C **47** 45 (2006).
- [15] K.M. Watson, Phys. Rev. Phys. Rev. **88** 1163 (1952).
- [16] M. Ablikim *et al.*, BES 2 Collaboration Phys. Lett. B **598** 149 (2004).

- [17] M. Ablikim *et al.*, BES 2 Collaboration Phys. Lett. B **633** 681 (2006).
- [18] D.V. Bugg, Eur. Phys. J A **25** 107 (2005); erratum Eur. Phys. J A **26** 151 (2005).
- [19] I. Caprini, G. Colangelo and H. Leutwyler, Phys. Rev. Lett. **96** 132001 (2006).
- [20] S. Descotes-Genon and B. Moussallam, Eur. Phys. J C **48** 553 (2006).
- [21] D.V. Bugg, J. Phys. G **35** 075005 (2008).
- [22] D.V. Bugg, Phys. Rev. D **78** 074023 (2008).
- [23] D. Aston *et al.*, LASS Collaboration, Nucl. Phys. B **296** 493 (1988).
- [24] D.V. Bugg, Phys. Lett. B **632** 471 (2006).
- [25] Particle Data Group, Phys. Lett. B **667** 1 (2008).
- [26] J.M. Link *et al.*, FOCUS Collaboration, Phys. Lett. B **653** 1 (2007).
- [27] G. Bonvicini *et al.*, CLEO C Collaboration, Phys. Rev. D **78** 052001 (2008).
- [28] V. Bernard, N. Kaiser and U.-G Meißner, Nucl. Phys. B **357** 129 (1991).
- [29] J.A. Oller, Phys. Rev. D **71** 054030 (2005).
- [30] E. van Beveren, D.V. Bugg, F. Kleefeld and G. Rupp, Phys. Lett. B **641** 265 (2006).
- [31] E. van Beveren *et al.* Z. Phys. C **30** 615 (1986).
- [32] R.L. Jaffe, Phys. Rev. D **15** 267 (1977).
- [33] A. Alboteanu, W. Kilian and J. Reuter, JHEP **10** 0811 (2008).